Early Detection of Oleic Acid-Induced Lung Injury in Rats Using ^{111}In-Labeled Anti-Rat Intercellular Adhesion Molecule-1

Ronald E. Weiner, Daniel E. Sasso, Maria A. Gionfriddo, Roger S. Thrall, Sergei Syrbu, Henry M. Smilowitz, and John Vento

Departments of Diagnostic Imaging and Therapeutics, Medicine, Surgery, and Pharmacology, University of Connecticut Health Center, Farmington; and Department of Radiology, VA Medical Center, Newington, Connecticut

Previous study of the bleomycin-induced lung injury model suggested that ^{111}In-labeled antirat intercellular adhesion molecule-1 (aICAM-1) might be a useful acute respiratory distress syndrome (ARDS) diagnostic agent. We further investigated the ability of ^{111}In-aICAM-1 to detect inflammation in another ARDS lung injury model. **Methods:** ^{111}In-labeled rat polymorphonuclear leukocytes (PMNs), ^{111}In-aICAM-1, ^{111}In-labeled normal mouse IgG (nmIgG), and ^{111}In-labeled rat serum albumin (RSA) were injected into rats 18–24 h before kill. Biodistributions, scintigraphic images, and lung ICAM-1 upregulation were obtained in uninjured rats and in rats after injury with oleic acid. **Results:** ^{111}In-RSA and ^{111}In-nmIgG localized in inflamed lung at 5 min postinjury (PI). ^{111}In-PMN uptake increased significantly only at 24 h PI. ^{111}In-aICAM-1 localization increased significantly (30%–60%) at 1 h PI and remained elevated up to 24 h PI. Lung/blood ratios (L/B) at 1 and 4 h PI were very low ($<$0.6) for ^{111}In-nmIgG and ^{111}In-PMN rats; however, for ^{111}In-aICAM-1 rats, they were $>$1 and 25%–60% higher than those for the control samples. A low L/B suggests poor inflammation detection on the images. Images and region-of-interest analysis confirmed that only ^{111}In-aICAM-1 could distinguish inflamed lungs at 4 h PI. ICAM-1 was upregulated at 4 and 24 h PI. **Conclusion:** In this model, ^{111}In-aICAM-1 detected lung inflammation very early in the course of the disease. These results support the suggestion that ^{111}In-aICAM-1 could be a very early, highly specific ARDS diagnostic agent and may be useful to detect a wide range of inflammations.

Key Words: inflammation; acute respiratory distress syndrome; adhesion molecules; inflammation imaging; immunoscintigraphy

J Nucl Med 2001; 42:1109–1115

Acute respiratory distress syndrome (ARDS) represents a group of diseases that have the common pathologic manifestation of acute diffuse lung injury. Its estimated incidence ranges from 8 to 75 people per 100,000, and it is associated with a mortality rate of 36%–60% (*1–3*). In many instances, multi-organ system failure follows the acute lung injury phase and is typically the primary cause of death. The most common cause of ARDS, accounting for 37%–45% of all cases, is gram-negative sepsis (*2–4*). Also, fat emboli from major bone fractures in some patients (approximately 25%) can cause direct pulmonary injury that leads to ARDS (*3*). The syndrome typically arises 24–72 h after the inciting incident (*5*). This period provides an opportunity to identify those patients in whom ARDS may develop, and it also provides time to begin prophylactic therapy. No specific therapy has been found to be beneficial; instead, the patient is managed in terms of respiratory, circulatory, and nutritional support (*2,6*). Recently, several new treatments, including inhaled nitrous oxide (*7*), instilled surfactant (*8*), and interleukin-1 receptor antagonist (*9*) have been attempted with ARDS and related disorders, but they have achieved little improvement in patient survival.

The mechanisms involved in the pathogenesis of ARDS are undoubtedly numerous, complex, and poorly understood (*2*). Various cells and mediators have been implicated (*10–13*). It is very difficult to establish whether a cell type or mediator precedes injury, causes injury, or is a secondary manifestation of that injury. Certainly, polymorphonuclear leukocytes (PMNs) have been shown to be present in high numbers in the lungs of patients with ARDS (*14,15*) and in animal models of ARDS (*16,17*) and have thus been implicated in the pathogenesis of the disease. Complicating the role of PMNs in ARDS is the observation that ARDS develops in neutropenic patients (*18*). Nevertheless, many studies of patients and animal models either directly or indirectly implicate PMNs (or their products) in the pathogenesis of ARDS. Investigators have been looking for clinical predictors of ARDS and have considered various mediators and cells without much success (*19–22*).

A hallmark of an acute infection/inflammation is the invasion of the site by large numbers of PMNs. A critical component of this directed movement is the ability of the PMNs to marginate in the blood vessels near the inflammation. An essential margination component is the expression

Received Oct. 12, 2000; revision accepted Mar. 8, 2001.

For correspondence or reprints contact: Ronald E. Weiner, PhD, Division of Nuclear Medicine, University of Connecticut Health Center, MC-2804, 263 Farmington Ave., Farmington, CT 06030.

of adhesion molecules, namely, intercellular adhesion molecule-1 (ICAM-1) on endothelial cells and its counter-receptor, leukocyte function antigen-1 (LFA-1), on the neutrophil surface (*23*,*24*). The interaction of LFA-1 and ICAM-1 allows the PMNs to become firmly attached to the endothelial cell. LFA-1 is expressed at low basal levels but is upregulated by a variety of proinflammatory agents. ICAM-1 is expressed constitutively and is also upregulated by various proinflammatory agents. The upregulation of ICAM-1 is usually long lasting with a maximum at 8–10 h and remains elevated for 2–7 d. This finding suggests that an antibody to ICAM-1 has the potential to be an early and specific inflammation detection agent, because ICAM-1 upregulation precedes PMN localization and remains elevated.

^{99m}Tc- and ^{111}In-labeled white blood cells (WBCs) are commonly used for acute inflammation detection and could be useful to identify patients in whom ARDS may develop. However, these agents are not without limitations (*25*,*26*). The preparation of each agent is very labor intensive (2–3 h) and requires specialized equipment. In addition, most community hospitals lack the expertise for such preparation and send the autologous blood to a commercial radiopharmacy for labeling, which adds an additional 1–2 h. Although imaging with ^{99m}Tc-WBCs can be performed within 1–4 h after injection, the rapid excretion of ^{99m}Tc into the bowel and the particularly transient uptake in the lung complicate inflammation detection in these areas. Thus, many laboratory and clinical studies are looking for a suitable replacement (*26–28*). Most of the agents being studied are targeted against antigens present on PMNs and thus dependent on an increased concentration of PMNs at the inflammatory site (*26*). We propose that ^{111}In-labeled mouse monoclonal anti-human ICAM-1 antibody (hum-aICAM-1) may be able to detect events in this disease even earlier than other agents because ICAM-1 upregulation precedes PMN localization. Thus, ^{111}In-hum-aICAM-1 could provide a highly specific, less expensive, and earlier means of inflammation detection. We showed previously in bleomycin-induced lung injury that the inflammation can be detected as early as 4 h after initiation (*29*).

In this study, we investigated the ability of ^{111}In-labeled mouse antirat ICAM-1 antibody (aICAM-1) to detect inflamed lung in the oleic acid (OA) model of fat emboli–induced lung injury. This agent was compared with ^{111}In-PMNs, which are the current standard agent, and ^{111}In-labeled rat serum albumin (RSA) and ^{111}In-labeled normal mouse polyclonal IgG (nmIgG), two markers of endothelial integrity.

MATERIALS AND METHODS

OA Model of Lung Injury

CDF:(F344)ClrlBR Fischer rats (Charles River Laboratories, Worthington, MA) were anesthetized, and each animal was injected intravenously with 300 μL of a suspension of OA (Sigma Chemical Co., St. Louis, MO). The suspension comprised 30 μL pure OA suspended in 270 μL 0.1% bovine serum albumin (*30*). Sham-injury (uninjured) animals received an injection of an equal volume of saline.

Preparation of ^{111}In-Labeled Proteins

The coupling of cyclic anhydride diethylenetriaminepentaacetic acid (DTPA) to aICAM-1 (Seikagaku Corp., Tokyo, Japan), nmIgG (Sigma Chemical Co., St. Louis, MO), or RSA (Sigma Chemical Co., St. Louis, MO) and the addition of ^{111}In (NEN Life Science Products, Boston, MA) to the protein-DTPA complex were performed as described previously (*31*). Each protein was conjugated with 0.8–1.3 DTPA/molecule, and DTPA conjugation had no significant effect on immunoreactivity.

Preparation of ^{111}In-PMNs

PMNs were harvested by lavage of the peritoneal cavity of normal rats with 60 mL heparinized saline (2 U/mL) 16 h after the intraperitoneal injection of 0.1% glycogen (20 mL in saline) (*32*). This method consistently yielded $>1 \times 10^8$ PMNs per animal with a purity >95%. ^{111}In-oxine, approximately 18.5 MBq/10^6 cells, was added to the cell suspension and incubated for 20 min at room temperature, and labeled cells were separated by centrifugation. Labeling efficiency averaged 70%–80%, and cell viability was always >85% as tested by the eosin-dye exclusion test.

Biodistribution of ^{111}In Radiopharmaceuticals in OA Model of Lung Injury

Rats (3 per group) received an intravenous injection of 1×10^8 ^{111}In-PMNs containing 370 kBq at 18–24 h before their scheduled kill time. OA was injected at 15 min, 30 min, 1 h, 4 h, 24 h, and 72 h before kill. Also, rats (3 or 4 per group) were injected intravenously with 111–222 kBq radioactivity containing 10 μg ^{111}In-nmIgG, ^{111}In-RSA, or ^{111}In-aICAM-1. For ^{111}In-nmIgG and ^{111}In-RSA, the radioactivity was injected at 18–24 h, and OA was injected at 5 min, 15 min, 30 min, 1 h, 4 h, 24 h, and 72 h (RSA only) before kill. The 5-min OA injection time was chosen because that is before detectable lung injury, and the 72-h OA injection time was chosen because that is when the lung injury begins to resolve spontaneously (*30*,*33*). For the ^{111}In-aICAM-1 experiments, the antibody was injected at 24 h and OA was injected at 1, 4, and 24 h before kill. This injury and biodistribution protocol was used previously with bleomycin (Fig. 1) (*27*). In the uninjured rats,

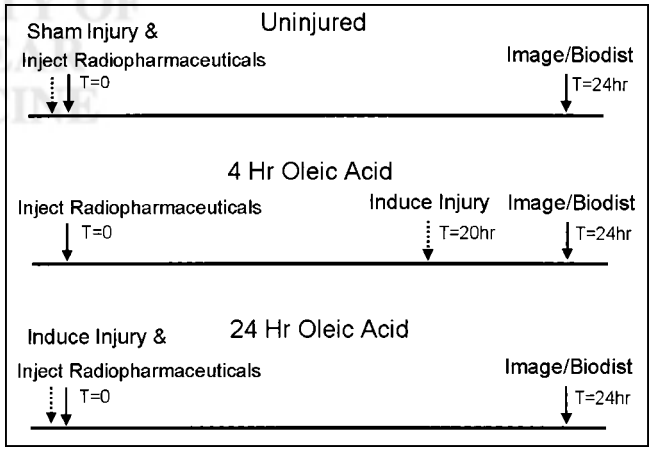

FIGURE 1. Experimental time line for injection of ^{111}In-labeled radiopharmaceuticals (solid arrow), injury with OA or sham injury (dotted arrow), and imaging or biodistribution (solid arrow) of rats. Only 2 injury times, 4 and 24 h, are shown for clarity.

a sham injection with saline was performed concurrent with the ^{111}In-labeled radiopharmaceutical injection. Generally, experiments were performed with 2 or 3 time points and a control group. The data were then combined using each control group as a reference, and a percentage for the control group was computed. At the time of the kill, whole organs and tissues were removed and weighed, and the radioactivity was measured (*31*). Data were computed as both percentage injected dose per gram of tissue (%ID/g) and percentage injected dose per organ (%ID/O).

When the data were analyzed for each radiopharmaceutical, we observed a consistently larger injury-induced increase in the %ID/O values compared with %ID/g values in the lung. We hypothesized that in this acute lung injury model, the inflammatory process caused a rapid accretion of fluid in the lungs. Any fluid increase would reduce any increase in %ID/g compared with %ID/O for these labeled compounds. For each labeled molecule, approximately a doubling of lung weight occurred, which peaked at 30 min–1 h PI ($P < 0.001$, compared with the uninjured lung) and then declined. This waxing and waning followed the course of the injury in this model (*30*). In all subsequent data, only %ID/O was compared because of this injury-induced lung weight increase. These data also showed that fluid influx was extremely rapid after the initiation of injury.

Imaging

Rats were imaged in the supine position at 24 h after injection of approximately 1.85 MBq containing 10 μg of sterile filtered ^{111}In-labeled proteins or 0.5×10^8 ^{111}In-PMNs, suspended in 0.5 mL saline (*31*). Briefly, anterior views of the upper torso using a pinhole collimator were obtained at 4 and 24 h PI as described above, and 100,000 counts were collected (Fig. 1). To obtain a quantitative estimate of organ and tissue localization, regions of interest (ROIs) were drawn around organs and tissue background. The counts per pixel from the ROIs were corrected for background and ^{111}In decay and divided by the acquisition time and injected dose for normalization.

Immunofluorescence of Lung Tissue

Lungs from rats at 4 and 24 h PI were excised, frozen in liquid nitrogen, cryostat sectioned, and assayed for the presence of ICAM-1 immunofluorescence as described previously (*29*).

Statistical Analysis

A one-way ANOVA with the Newman–Keuls test was applied to compare the effect of time PI for the labeled radiopharmaceuticals and to compare the different radiopharmaceuticals at the same time (*34*).

RESULTS

Uptake of ^{111}In-PMNs, ^{111}In-aICAM-1, ^{111}In-nmIgG, and ^{111}In-RSA in OA-Injured Rats

Figure 2 shows the uptake in injured lung for two labeled proteins, which are indicators of endothelial permeability. The uptakes of ^{111}In-nmIgG and ^{111}In-RSA in the lung increased dramatically two- to threefold at 5 min and were similar until 24 h (Fig. 2). Lung function measurements (*33*) and histology (*30*) indicate lung damage 15 min after injection of OA. At 24 h, ^{111}In-RSA in the lung declined ($P < 0.005$, vs. 4 h). In contrast, ^{111}In-nmIgG uptake doubled ($P < 0.001$, vs. 4 h). Injury did not cause the presence of

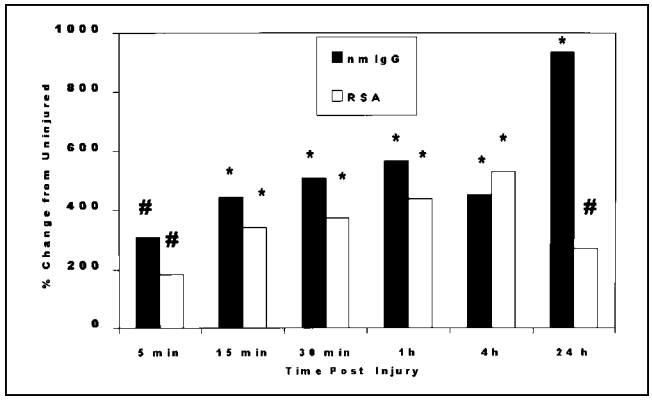

FIGURE 2. Effect of time after OA injury on lung uptake of ^{111}In-RSA and ^{111}In-nmIgG. Data are given as percentage change compared with uninjured lung using %ID/O values (#, $P < 0.05$; *, $P < 0.001$).

^{111}In in other tissues to change except in the kidney (for ^{111}In-nmIgG), which showed a modest but significant decline, and in the blood (for ^{111}In-RSA), which was elevated modestly in activity as the injury progressed (data not shown). These data show that endothelial leakiness can be detected as early as 5 min PI in this model.

Although the endothelial barrier was disrupted, no significant increase in ^{111}In-PMN lung uptake occurred until 24 h PI (Fig. 3). At that time, a dramatic, approximately 25-fold increase occurred, compared with the control uninjured lung. In contrast, at 1 h PI, rats injected with ^{111}In-aICAM-1 had a modest but significant increase in lung activity, which increased at 24 h. No significant change in ^{111}In-PMN uptake occurred in most other tissues after the lung injury initiation. The exception was in the spleen, where a significant, approximately 50% reduction occurred, compared with the uninjured value, only at 24 h (data not shown). This reduction would be consistent with recruitment of PMNs from the spleen to other tissues, particularly the lung, at 24 h. Also, kidney activity increased significantly at 4 h and remained elevated (26%–50%) (data not shown). For ^{111}In-aICAM-1, the kidney was also the only tissue that showed a consistent significant increase in antibody accumulation as a function of injury (data not shown).

Lung-to-Tissue Ratios

The data from Figures 2 and 3 suggest that ^{111}In-nmIgG would be an excellent early inflammation detection agent because of the high early uptake (5 min to 4 h); ^{111}In-aICAM-1 and ^{111}In-PMNs would be poor in comparison. However, this finding does not take into account that target detection is dependent on the ratio of the target (in this case, the lung) to the tissue background. To estimate the detection ability of each agent, a ratio was computed using different tissue backgrounds that could interfere with the detection of lung inflammation (Fig. 4). Thus, target detection is based on the increase of the ratio from the uninjured value. Animals injected with ^{111}In-PMNs showed only at 24 h a

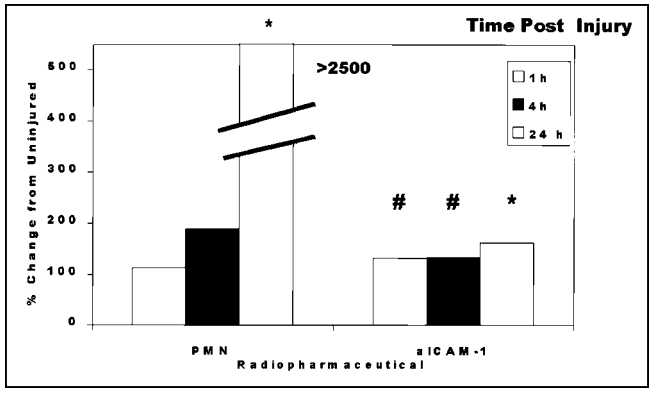

FIGURE 3. Effect of time after OA injury on lung uptake of ^{111}In-PMNs and ^{111}In-aICAM-1. Data are given as percentage change compared with uninjured lung using %ID/O values (#, $P < 0.05$; *, $P < 0.001$).

significantly high lung-to-blood ratio (L/B), which is consistent with the results shown in Figure 3. This high L/B was mainly a result of low blood activity (approximately 1 %ID/O) and suggests that inflammation detection by imaging would be likely only at 24 h PI.

The ^{111}In-aICAM-1 results, which showed a modest injury-induced increase in lung activity, showed a large increase (not quite significant) in L/B at 1 h PI (Fig. 4). More importantly, the early (1 and 4 h) L/B and lung-to-heart ratios (L/H) were >1; the L/B was sixfold ($P < 0.001$) and the L/H was twofold ($P < 0.001$) greater than the comparable ^{111}In-nmIgG values. This result was caused primarily by very low blood and heart uptake, 5 and 0.2 %ID/O, respectively, at this time PI. Even at 24 h, the ^{111}In-aICAM-1 L/B was still approximately threefold (P = not significant) greater than the ^{111}In-nmIgG value. This finding suggests that the injured lung might be detected visually as early as 4 h PI with ^{111}In-aICAM-1.

However, in the ^{111}In-nmIgG-injected rats, although the ratios increased significantly very early in the injury progression (1 h) (Fig. 4), the L/B was very low, <0.2 (Fig. 4A). Although a large increase was seen at 1–4 h PI, the low L/B suggests that the high blood background (27 %ID/O) could obscure the injured lung. Thus, in this early time frame, ^{111}In-aICAM-1 could be a better imaging agent compared with ^{111}In-nmIgG. As injury progressed to 24 h, both ratios for ^{111}In-nmIgG-injected rats doubled at 24 h PI (>4 h, $P < 0.001$) (Fig. 4). This result suggests that the injured lung might be detectable at this time, because the blood activity was reduced to 20 %ID/O.

Imaging of ^{111}In-PMNs, ^{111}In-aICAM-1, and ^{111}In-nmIgG in OA-Injured Rats

The imaging of these radiopharmaceuticals generally followed what we observed in the tissue ratio data. Figure 5 shows the deposition of these compounds at 4 and 24 h PI with OA. In the upper-torso images of uninjured rats injected with ^{111}In-PMNs, only the intense uptake in the liver can be detected. At 4 h PI, the lung uptake was no greater than the tissue background, but liver activity remained. As the injury progressed to 24 h, activity is clearly apparent and well defined in both lungs.

In the uninjured animals, ^{111}In-aICAM-1 localized mainly in the liver, and some activity was seen in the lung fields. In contrast to the ^{111}In-PMN images, the 4-h ^{111}In-aICAM-1 images of the injured rat show that the lung fields are visible, defining the cardiac shadow (Fig. 5). Activity was also present in the liver. At 24 h, although no change in liver activity was seen, activity in the lung clearly defined the 2 lung lobes. The tissue background, although not as low as ^{111}In-PMNs, is lower than that visible in the ^{111}In-nmIgG images. Also, little activity is seen in the bone or bone marrow in any of the images. Thus, ^{111}In-aICAM-1 can detect lung injury earlier than ^{111}In-PMNs, which was suggested by the tissue ratios (Fig. 4).

The image of the ^{111}In-nmIgG uninjured rat showed only cardiac blood and liver activity and very little lung activity. At 4 h PI, the image showed a high concentration of activity in the cardiac blood pool (Fig. 5). Although the lung fields

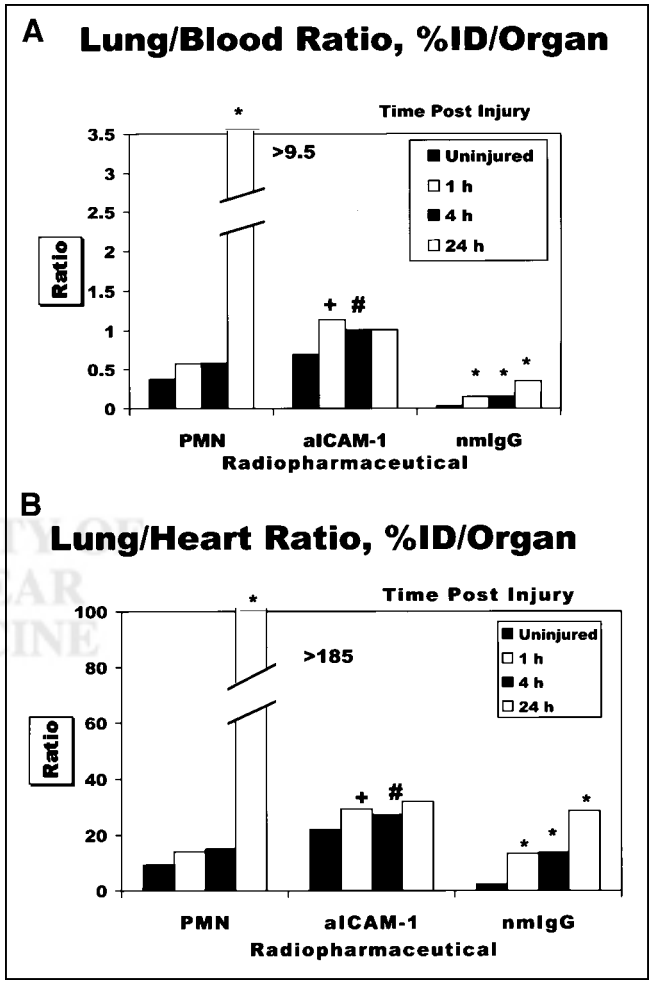

FIGURE 4. Effect of time after OA injury on L/B (A) and L/H (B) for ^{111}In-PMNs, ^{111}In-aICAM-1, and ^{111}In-nmIgG. Data were computed using %ID/O values (*, $P < 0.001$; +, $0.05 < P < 0.1$; #, $P < 0.05$).

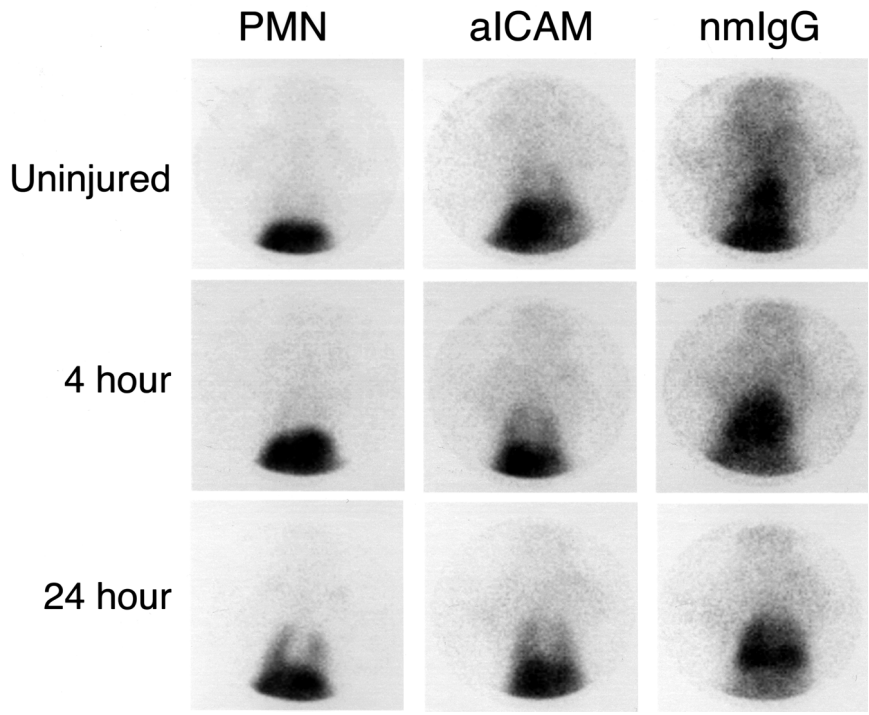

FIGURE 5. Pinhole scintigrams of upper anterior torso of uninjured rats and rats at 4 and 24 h after OA injury injected with ^{111}In-PMNs, ^{111}In-aICAM-1, or ^{111}In-nmIgG. Animals were imaged at 24 h after injection with GE gamma camera (General Electric, Milwaukee, WI).

were not well defined, the activity in the lungs appeared higher than the tissue background. Liver activity, although higher than background, is not nearly as intense as the cardiac blood pool. As injury progressed (24 h), the activity in the lung field intensified. The most intense areas appeared to be in the lung bases, and some activity was seen in the upper lobes. The cardiac blood at 24 h PI was not nearly as intense as at 4 h and can be distinguished from the lungs. Liver uptake was lower than the lungs and similar to the uptake in the 4-h image. These images are consistent with the predictions from the tissue ratio data.

To obtain quantitative information from the images, a ROI analysis was performed. Table 1 shows that for ^{111}In-PMNs, a modest 40% increase in lung count density occurred at 4 h compared with the uninjured animals. In contrast, a 500%–600% significant enhancement occurred

TABLE 1
Effect of OA-Induced Lung Injury on ROI Analysis of Rats Injected with ^{111}In-Labeled Agents

Injected agent	ROI	Uninjured	4 h PI	24 h PI
^{111}In-PMNs	Left lung	8.81 ± 2.49	12.78 ± 0.19*	45.54 ± 3.49†
	Right lung	9.89 ± 2.92	14.03 ± 0.76	58.95 ± 5.30†
	Both lungs‡	9.35 ± 2.70	13.41 ± 0.46	52.24 ± 4.41†
	Liver	151.46 ± 32.65	245.89 ± 21.43†	185.51 ± 9.35*
	Heart	7.41 ± 1.27	12.05 ± 0.41*	26.81 ± 3.14†
^{111}In-aICAM-1	Left lung	8.30 ± 1.19	16.81 ± 0.86†	32.92 ± 1.27†
	Right lung	9.32 ± 1.38	19.41 ± 0.73†	40.95 ± 3.14†
	Both lungs‡	8.81 ± 1.27	18.11 ± 0.81†	36.92 ± 2.19†
	Liver	44.32 ± 1.65	65.81 ± 2.38†	92.35 ± 2.92†
	Heart	7.68 ± 0.41	13.70 ± 0.70†	20.19 ± 0.65†
^{111}In-nmIgG	Left lung	15.22 ± 1.59	38.59 ± 0.59†	54.78 ± 2.32†
	Right lung	14.65 ± 1.22	37.38 ± 0.84†	63.24 ± 2.30†
	Both lungs‡	14.95 ± 1.41	38.00 ± 0.70†	59.00 ± 2.30†
	Liver	20.78 ± 0.86	25.86 ± 0.97†	28.03 ± 0.84†
	Heart	21.46 ± 0.51	37.08 ± 0.97†	60.97 ± 0.95†

*$P < 0.05$, compared with uninjured.
†$P < 0.001$, compared with uninjured.
‡$n = 10$; all others, $n = 5$.
Values are $\times 10^{-4}$ mean ± SD, given as cpm/pixel/kBq.

at 24 h. Lung activity was comparable with heart activity in the uninjured rat and at 4 h PI. However, at 24 h PI, the lung count density was double the heart activity when the lungs were clearly visible. In contrast, lung values from the ^{111}In-aICAM-1-injected animals increased significantly (200%) at 4 h. More important, the lung count density was approximately 30% greater than the heart value at this time, and this relationship improved at 24 h (approximately 180% greater). Although lung cpm/pixel values in ^{111}In-nmIgG rats were elevated significantly as early as 4 h, heart and liver values were comparable. This finding explains why it was difficult to detect the inflamed lungs.

Expression of ICAM-1 on Lung Tissue

Previous data showed that ICAM-1 was upregulated as early as 30 min PI (*33*). Figure 4 shows that ICAM-1 remains upregulated at 4 h (Fig. 6C) and 24 h (Fig. 6E) PI; the increased fluorescence intensity is apparent in the injured lung compared with lung tissue from uninjured rats (Fig. 6A). Control experiments with no added aICAM-1 showed no fluorescence intensity from either uninjured or injured lung tissue (Figs. 6B, 6D, and 6F).

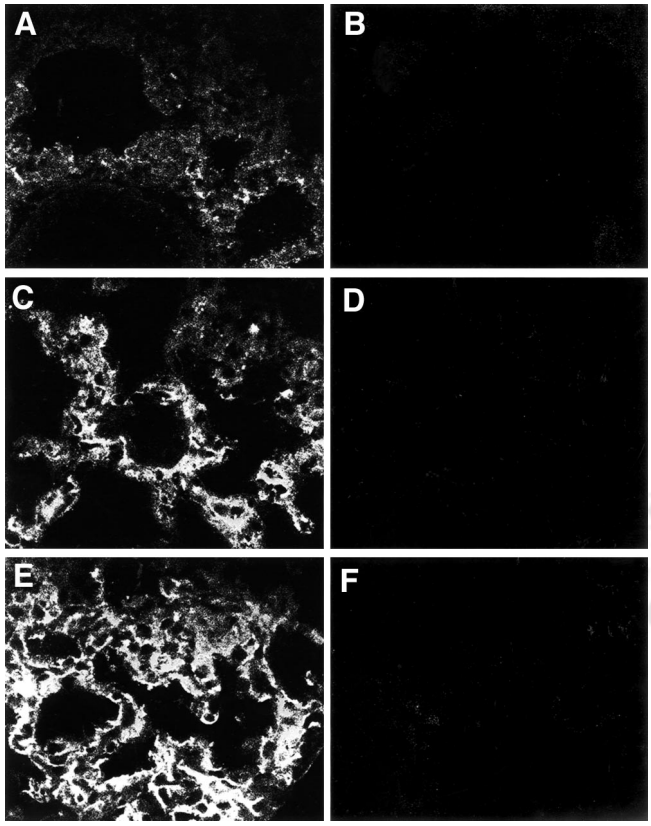

FIGURE 6. Expression of ICAM-1 immunofluorescence in cryostat sections of OA-injured and uninjured rat lung. Sections were processed for immunofluorescence using aICAM-1 as first antibody in lung from uninjured rat (A), rat injured at 4 h (C), and 24 h before kill (E). For control samples, no aICAM-1 was used as first antibody in lung from uninjured rat (B), rat injured at 4 h (D), and 24 h before kill (F). Rhodamine-conjugated goat anti-mouse IgG was used as second antibody in all sections (magnification, ×788).

DISCUSSION

Our data suggest that ^{111}In-aICAM-1 is a useful indicator of acute inflammation development in this model. Images showed that inflamed lungs could be detected very early (4 h PI) in the course of injury. The 24-h images were somewhat better. This result was consistent with biodistribution data, target-to-background ratios, and ROI analysis. Some data even suggested that ^{111}In-aICAM-1 may detect injury as early as 1 h PI. Although ^{111}In-nmIgG localized extremely early (within 5 min) in injured tissue, it was difficult to detect the inflamed lung in the scintigraphic images because of high blood-pool activity in the heart. In contrast, ^{111}In-PMNs, which are the currently used acute inflammation detection agent, could not detect inflamed lungs until the injury had progressed at least 24 h in this model.

Our data also show that ^{111}In-aICAM-1 is highly specific. ^{111}In-aICAM-1 localization was increased as early as 1 h PI and remained elevated at our latest data point (24 h). A previous study showed that ICAM-1 is upregulated at 30 min PI in this model (*33*). The immunofluorescence data presented in this study show that ICAM-1 remained upregulated as long as 24 h PI. If ^{111}In-aICAM-1 localization was related solely to injury-induced endothelial barrier disruption, we would expect very early and high lung uptake. For example, both ^{111}In-nmIgG and ^{111}In-RSA uptake increased dramatically as early as 5 min PI and peaked at 1 h PI, and these values were 568% and 440% greater, respectively, than those for the uninjured lung (Fig. 2). However, the lung uptake of ^{111}In-aICAM-1, even at 1 h, was rather modest (32% increase) (Fig. 3). Thus, the likely driving force for ^{111}In-nmIgG and ^{111}In-RSA lung uptake was the high blood concentration (approximately 20–27 %ID/O) combined with the endothelial barrier disruption. In contrast, the low blood concentration (4–5 %ID/O) of ^{111}In-aICAM-1 most likely required an active process, namely, ICAM-1 upregulation, for localization. We showed the high specificity of this labeled antibody in another model of lung injury (*29*). However, in this model, the injury-induced endothelial barrier disruption preceded ICAM-1 upregulation.

We propose using ^{111}In-hum-aICAM-1 in patients at risk for ARDS similarly as it was used in this study. In patients at a high risk for ARDS, there appears to be a 24–72 h period after the inciting incident during which ARDS may develop (*5*). The labeled antibody would be injected, and the patient would be imaged sequentially over the next 72 h. Our data suggest that although little human ^{111}In-aICAM-1 would be circulating, lungs that became inflamed would be detected readily as early 4 h but at least within 24 h. Imaging up to 72 h might be possible, because beyond 4 h after injection, ^{111}In-aICAM-1 disappears very slowly (*31*). Although no therapeutic intervention has been found to be effective, with this early-detection method, interventions could be started and tested in the earliest stages of the disease.

^{111}In-hum-aICAM-1 has several advantages over the existing agents. The preparation is simple and requires only the addition of ^{111}In. This choice would eliminate the preparation problem associated with both ^{111}In- and ^{99m}Tc-labeled WBCs. Blood handling is unnecessary. If the animal data can be translated to humans, we would expect a low constant lung uptake and very low uptake in bone, bone marrow, and intestines. This situation would make inflammation detection in these areas much easier. Studies are in progress to attach ^{99m}Tc to aICAM-1, which could further improve this agent and make it useful to detect a wide array of inflammations (*35*). The half-life for ^{99m}Tc is consistent with the localization time frame for this antibody.

CONCLUSION

We have developed a labeled antibody that takes advantage of the role of adhesion molecules in the inflammatory process. This new radiopharmaceutical localizes rapidly with high specificity in two animal models of lung inflammation. This compound has the potential to rapidly diagnose ARDS and other inflammatory processes to allow early therapeutic interventions. Whether this potential will be realized must await patient trials.

ACKNOWLEDGMENTS

This research was supported in part by faculty research grants from the University of Connecticut Health Center.

REFERENCES

1. Murray JF, Matthay MA, Luce JM, Flick MR. An expanded definition of adult respiratory distress syndrome. *Am Rev Respir Dis.* 1988;138:720–723.
2. Ware L, Matthay, MA. The acute respiratory distress syndrome. *N Engl J Med.* 2000;342:1334–1349.
3. Milberg JA, Davis DR, Steinberg KP, Hudson LD. Improved survival of patients with acute respiratory distress syndrome (ARDS): 1983–1993. *JAMA.* 1995;273: 306–309.
4. Martin MA, Silverman HJ. Gram-negative sepsis and the adult respiratory distress syndrome. *Clin Infect Dis.* 1992;14:1213–1228.
5. Hudson LD, Milberg JA, Anardi D, Maunder RJ. Clinical risks for development of the acute respiratory distress syndrome. *Am J Respir Crit Care Med*. 1995; 151:293–301.
6. Stevens JH, Raffin TA. Adult respiratory distress syndrome. II. Management. *Postgrad Med J.* 1984;60:573–576.
7. Rossaint, R, Falke KJ, Lopez F, Slama K, Pison U, Zapol WM. Inhaled nitric oxide for the adult respiratory distress syndrome. *N Engl J Med.* 1993;328:399–405.
8. Anzueto A, Baughman RP, Guntupalli KK, et al. Aerosolized surfactant in adults with sepsis-induced acute respiratory distress syndrome. *N Engl J Med.* 1996; 334:1417–1421.
9. Fisher CJ Jr, Dhainaut JF, Opal SM, et al. Recombinant human interleukin-1 receptor antagonist in the treatment of patients with sepsis syndrome: results from a randomized, double-blind, placebo-controlled trial. *JAMA.* 1994;271:1836–1843.
10. Jacobs RF, Tabor DR, Burks AW, Campbell GD. Elevated IL-1 release by human alveolar macrophages in ARDS. *Am Rev Respir Dis.* 1989;140:1686–1692.
11. Hyers, TM, Tricomi SM, Dettenmeier PA, Fowler AA. TNF levels in serum and bronchoalveolar lavage fluid of patients with the adult respiratory distress syndrome. *Am Rev Respir Dis*. 1992;144:268–271.
12. Madtes, DK, Rubenfeld G, Klima LD, et al. Elevated transforming growth factor-levels in bronchoalveolar lavage fluid of patients with acute respiratory distress syndrome. *Am J Respir Crit Care Med.* 1998;158:424–430.
13. Nash, JRG, McLaughlin PJ, Hoyle C, Roberts D. Immunolocalization of tumor necrosis factor α in lung tissue from patients dying with adult respiratory distress syndrome. *Histopathology.* 1991;19:395–402.
14. Fowler AA, Hyers TM, Fisher BJ, Bechard DE, Centor RM, Webster RO. ARDS: cell populations and soluble mediators in the air spaces of patients at high risk. *Am Rev Respir Dis*. 1987;136:1225–1231.
15. Powe JE, Short A, Sibbald WJ, Driedger AA. Pulmonary accumulation of polymorphonuclear leukocytes in the adult respiratory distress syndrome. *Crit Care Med*. 1982;10:712–718.
16. Eiermann GJ, Dickey BF, Thrall RS. Polymorphonuclear leukocyte in acute oleic-acid-induced lung injury. *Am Rev Respir Dis*. 1983;128:845–850.
17. Haslett C, Worthen GS, Giclas PC, Morrison DC, Henson JE, Henson PM. The pulmonary vascular sequestration of neutrophils in endotoxemia is initiated by an effect of endotoxin on the neutrophil in the rabbit. *Am Rev Respir Dis*. 1987; 136:9–18.
18. Braude S, Apperley J, Krautz T, Goldman JM, Royston D. Adult respiratory distress syndrome after allogenic bone-marrow transplantation: evidence for a neutrophil-independent mechanism. *Lancet.* 1985;1:1239–1242.
19. Hammerschmidt D, Weaver L, Hudson LD, Craddock P, Jacob H. Association of complement activation and elevated plasma-C5a with the adult respiratory distress syndrome: pathophysiologic relevance and possible prognostic value. *Lancet.* 1980;1:947–949.
20. Zilow G, Joka T, Obertacke U, Rother U, Mirschfink M. Generation of anaphylatoxin C3a in plasma and bronchoalveolar lavage fluid in trauma patients at risk for the adult respiratory distress syndrome. *Crit Care Med*. 1992;20:468–473.
21. Donnelly SC, MacGregor I, Zamani A, et al. Plasma elastase levels and the development of the adult respiratory distress syndrome. *Am J Respir Crit Care Med*. 1995;151:1428–1433.
22. Sessler CN, Windsor AC, Schwartz M, et al. Circulating ICAM-1 is increased in septic shock. *Am J Respir Crit Care Med.* 1995;151:1420–1427.
23. Springer TA. Traffic signals for lymphocyte recirculation and leukocyte emigration: the multistep paradigm. *Cell*. 1994;76:301–314.
24. Carlos TM, Harlan JM. Leukocyte-endothelial adhesion molecules. *Blood*. 1994; 84:2068–2101.
25. Coleman RE, Datz FL. Detection of inflammatory disease using radiolabeled cells. In: Sandler MP, Coleman RE, Wackers F, Patton JA, Gottshalk A, Hoffer PB, eds. *Diagnostic Nuclear Medicine.* 3rd ed. Baltimore, MD: Williams & Wilkins; 1996:1509–1524.
26. Weiner RE, Thakur ML. Imaging infection/inflammations. *Q J Nucl Med.* 1999; 43:2–8.
27. Barron B, Hanna C, Passalaqua AM, Lamki L, Wegener WA, Goldenberg DM. Rapid diagnostic imaging of acute nonclassic appendicitis by leukoscintography with sulesomab, a technetium-99m-labeled antigranulocyte antibody Fab′ fragment: LeukoScan appendicitis clinical trial group. *Surgery*. 1999;125:288–296.
28. Kipper SL, Rypins EB, Evans DG, Thakur ML, Smith TD, Rhodes B. Neutrophil specific ^{99m}Tc-labeled anti-CD15 monoclonal antibody imaging for diagnosis of equivocal appendicitis. *J Nucl Med*. 2000;41:449–455.
29. Weiner RE, Sasso DE, Gionfriddo MA, et al. Early detection of bleomycin-induced lung injury in rat using ^{111}In-labeled antibody directed against intercellular adhesion molecule-1. *J Nucl Med.* 1998;39:723–728.
30. Dickey BF, Thrall RS, McCormick JR, Ward PA. Oleic acid-induced lung injury in the rat: failure of indomethacin treatment or complement depletion to ablate injury. *Am J Pathol*. 1981;103:376–383.
31. Sasso D, Gionfriddo M, Thrall R, Syrbu S, Smilowitz H, Weiner R. Biodistribution of ^{111}In labeled antibody directed against intracellular adhesion molecule-1 in normal rats. *J Nucl Med*. 1996;37:656–661.
32. Watts FL, Oliver BL, Johnson GM, Thrall RS. Superoxide production by rat neutrophils in the oleic acid model of lung injury. *Free Radical Biol Med*. 1990;9:327–332.
33. Syrbu S, Thrall RS, Wisniecki P, Lifchez S, Smilowitz HM. Increased immunoreactive rat lung ICAM-1 in oleic acid-induced lung injury. *Exp Lung Res.* 1995;21:599–616.
34. Zar JH. *Biostatistical Analysis.* Englewood Cliffs, NJ: Prentice-Hall; 1974:151–161.
35. Weiner R, Jacunski J, Sasso D, Theodoropulos S, Vyas R. Acute lung injury detection in rat models using Tc-99m labeled aICAM-1 [abstract]. *Nucl Med Commun*. 2000;21:596.